Available online at http://rjas.rsu.ac.th

Rangsit Journal of Arts and Sciences, July-December 2016 RJAS Vol. 6 No. 2, pp. 117-127

ISSN2229-063X (Print)/ISSN2392-554X (Online)

Experimental analysis on noise tolerance of bidirectional confidential with bilateral filter in local based optical flow for image reconstruction

Darun Kesrarat[1*] and Vorapoj Patanavijit[2]

[1]Department of Information Technology, Vincent Mary School of Science and Technology,
Assumption University, Samuthprakarn 10540, Thailand
Email: darunksr@gmail.com
[2]Department of Computer and Network Engineering, Vincent Mary School of Engineering,
Assumption University, Samuthprakarn 10540, Thailand
Email: patanavijit@yahoo.com

*Corresponding author

Submitted 2 July 2015; accepted in final form 14 October 2016
Available online 19 December 2016

Abstract

Noise is the main issue causing defects in the optical flow for motion prediction where the result in the motion vector (MV) is directly impacted. In this paper, we perform an experimental analysis on numerous noise tolerance models for a local based optical flow where the main model is bidirectional confidential with bilateral filter. For performance analysis, we focused on 2 main indicators. These are Structural SIMilarity (SSIM) and Error Vector Magnitude (EVM) where SSIM was used to indicate the quality for image reconstruction issues and EVM was used to indicate the accuracy in MV issues. In our experiments, the Additive White Gaussian Noise (AWGN) was formed at several noise levels over several standard sequences for performance evaluation.

Keywords: *optical flow, bilateral filter, bidirectional confidential, SSIM, EVM, AWGN.*

1. Introduction

In many fields such as super image reconstruction, movement detection and tracking, video compression and encoding, and visual odometry, the optical flow is one of the favored techniques used to compute the image velocity or the MV from different images in related time frames at every voxel position.

There are many domains in optical flow for MV determination such as phase based (Fleet & Jepson, 1990), block-based (Reed, 2005), local gradient based (Lucas & Kanade, 1981), and global gradient based (Horn & Schunck, 1981) where there are differences in the technique and environment where they are applied. But none of the techniques can produce efficient results when they are interfered by unintended factors such as noise.

Several noise tolerance models for the optical flow have been proposed such as gradient orientation information (Kondo & Kongpawechnon, 2009) and a bidirectional based optical flow (Kondo & Kongpawechnon, 2009; Kesrarat & Patanavijit, 2011a, 2013). One of the leading approaches is a bilateral filter (Sun, Li, Kang, & Shun, 2005; Paris, Kornprobst, Tumblin, & Durand, 2008; Mozerrov, 2013). Bilateral filter is a robust edge- preservation filter that is commonly applied in a computer vision and in image processing. The return of high reliability from bidirectional based optical flow (Kesrarat & Patanavijit, 2010) and under the performance investigation (Kesrarat & Patanavijit, 2011b) presents a high performance in reliability of MV over several models. Thus, our work is focused on the experimental analysis of a bidirectional confidential with a bilateral filter (Kesrarat & Patanavijit, 2015) and additionally under SSIM and EVM under an interfered AWGN environment.

AWGN is a basic noise standard used to represent random processes that appear in nature. In terms of noise interfered image, with Signal to Noise Ratio (SNR) in 3 different decibels (dB), contamination with 4 standard sequences was simulated in our experiment.

2. Objectives

As there are many application areas in optical flow, the result of optical flow can be applied for many purposes such as in the area of image restoration and image super image

reconstruction where the quality of the image is the main issue and in the area of motion detection/tracking in which the accuracy in velocity of MV is the important issue. The objective of this paper is to explain the impact of noise tolerance on local based optical flow models by using SSIM and EVM as indicators. SSIM index is a method for measuring the similarity between two images. EVM index is a measure of how far away the points are from their ideal locations.

3. Materials and methods

3.1 Lucas-Kanade optical flow (LK)

This algorithm uses the local based differential technique (Lucas & Kanade, 1981) by assuming the constant in local neighborhoods with least-square to solve the equation. For computation of gradient tension, the image velocity from spatiotemporal of image gradient (*G*) can be defined as:

$$G_x = \tfrac{1}{4}\{G(x,y+1,i) - G(x,y,i) + G(x+1,y+1,i) - G(x+1,y,i) + G(x,y+1,i+1) - G(x,y,i+1) + G(x+1,y+1,i+1) - G(x+1,y,i+1)\} \quad (1.1)$$

$$G_y = \tfrac{1}{4}\{G(x+1,y,i) - G(x,y,i) + G(x+1,y+1,i) - G(x,y+1,i) + G(x+1,y,i+1) - G(x,y,i+1) + G(x+1,y+1,i+1) - G(x,y+1,i+1)\} \quad (1.2)$$

$$G_f = \tfrac{1}{4}\{G(x,y,i+1) - G(x,y,i) + G(x+1,y,i+1) - G(x+1,y,i) + G(x,y+1,i+1) - G(x+1,y,i) + G(x+1,y+1,i+1) - G(x+1,y+1,i)\} \quad (1.3)$$

where *G(x,y,i)* implies the gradient tension (luminosity) in position *(x,y)* on the image at time *i* and assigns the weighted least-squares as a proper model over spatial neighbourhood for classifying MV. The equation is defined as:

$$\begin{bmatrix} u(x,y,i) \\ v(x,y,i) \end{bmatrix} = \begin{bmatrix} \sum G_x^2(x,y,i) & \sum G_x(x,y,i)G_y(x,y,i) \\ \sum G_x(x,y,i)G_y(x,y,i) & \sum G_y^2(x,y,i) \end{bmatrix}^{-1} \times \begin{bmatrix} -\sum G_x(x,y,i)G_t(x,y,i) \\ -\sum G_x(x,y,i)G_t(x,y,i) \end{bmatrix} \quad (2)$$

From Eq. 2, the first MV is classified and reiterated to classify the finishing MV. This algorithm leads to rapid computation and good noise tolerance but is weak in accuracy of velocity due to the concept of local based differential techniques.

3.2 Four-point central mask coefficient

The kernel of mask coefficient for computation in luminosity (Barron, Fleet, & Beauchemin, 1994) promotes more reliability in luminosity determination for local based optical flow.

This kernel (BFB kernel) adapts four-point mean differences (1/12 [-1 : 8 : 0 : -8 : 1]) for luminosity determination and it is defined as:

$$\begin{aligned} G_x &= 1/12\{-G_{x,y-2} + 8\times G_{x,y-1} + -8\times G_{x,y+1} + G_{x,y+2}\} \\ G_y &= 1/12\{-G_{x-2,y} + 8\times G_{x-1,y} + -8\times G_{x+1,y} + G_{x+2,y}\} \\ G_i &= 1/12\{-G_{x,y,i-2} + 8\times G_{x,y,i-1} + -8\times G_{x,y,i+1} + G_{x,y,i+2}\} \end{aligned} \quad (3)$$

3.3 Bidirectional based model (BD)

This algorithm (Li & Yu, 2008) is expressed in bidirection (MV of frame $i \rightarrow i+1$ and MV of frame $i+1 \rightarrow i$) to determine more reliability in MV. The confidence rate (*C*) to determine the reliability is calculated by using MV of both directions. The equation is defined as:

$$C_l^n(k,i) = \exp\left(-\frac{\| v_l^n(k,i) + v_{l^-}^n(k + v_l^n(k,i), i+1) \|}{\frac{(\| v_l^n(k,i) \| + \| v_{l^-}^n(k + v_l^n(k,i), i+1) \|)}{2+\beta}} \right) \quad (4)$$

where l is $i \rightarrow i+1$, l^- is $i+1 \rightarrow i$, β prevents invalid denomination by zero, and *k* implies current pixel.

Consequently, the finishing MV ($\bar{v}$ and $\bar{u}$) is calculated as an average of confidence based pre-defined locale (*L(k0)*). The equation is defined as:-

$$\bar{v}_l^n(k_0) = \frac{\left(\sum_{k_i \in L(s_0)} C_l^n(k_i)\bar{v}_l^n(k_i) \right)}{\left(\sum_{k_i \in L(s_0)} C_l^n(k_i) \right)} \quad (5)$$

This algorithm presents an excellent performance with reliable results in MV over numerous environments such as clear sequence and noise contamination sequences.

3.4 Bilateral filter (BF)

This bilateral filter is a well know robust edge- preservation filter that was assigned over extensive image processing, and computer vision (Sun et al., 2005, Paris et al., 2008; Mozerrov, 2013) defined as:-

$$\varphi(x+n) = \exp\left(\frac{|n|^2}{2\delta_a^2} + \frac{|G(x+n) - G(x)^2|}{2\delta_b^2} \right) \quad (6)$$

where δ_a implies the standard deviation of *v(x)* × *7* and δ_c implies the standard deviation of *G(x)*. The equation is expressed in correspondence with signal *u(x)* to determine MV.

A bilateral filter is utilized to compute the final MV as follows:-

$$v_b(x) = \frac{1}{Y} \sum_{|n|<N} v(x)\phi(x+n) \quad (7)$$

where $\phi()$ implies a bilateral Gaussian kernel, Y implies the kernel normalization factor, and n implies locale range and was set to ±3 in our experiment.

$$Y = \sum_{|n|<N} \phi(x+n) \quad (8)$$

3.5 Bidirectional confidential with bilateral filter (BB)

This algorithm (Kesrarat & Patanavijit, 2015) enjoins the bidirectional procedure in combination with the bilateral filter.

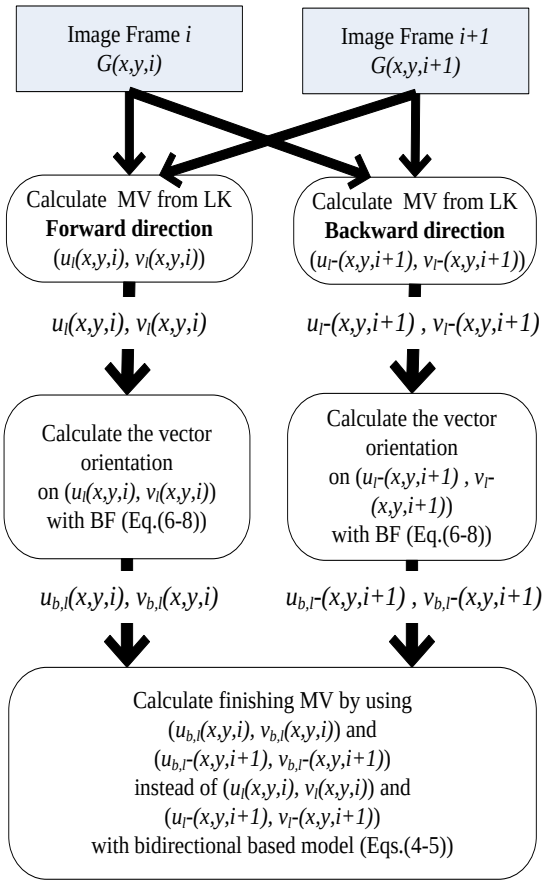

Figure 1 Process flow of BB

The interlink of the bilateral filter with a bidirectional confidential is adapted to promote higher performance in computation for more reliability in MV under the noisy state.

Firstly, the MV on both directional in $i \rightarrow i+1$ and $i+1 \rightarrow i$ are computed by traditional LK optical flow with BFB kernel (($u_{l,}$ v_l) and ($u_{l-,}$ v_{l-})). This process was further continued by assigning the bilateral filter on ($u_{l,}$ v_l) and ($u_{l-,}$ v_{l-}) for both directions as the unit vector orientation ($u_{b,}$ v_b). Finally, the confidence based model (Eq.4 and Eq.5) is assigned to compute the finishing MV by using the values of the unit vector orientation ($u_{b,}$ v_b) instead of traditional MV ($u_{,}$ v). The process flow for BB is represented in Figure 1.

4. Experimental analysis and performance comparison

In this research, a local based optical flow in the LK model with a four-point central mask coefficient is concentrated with robust reference models (BD, BF, and BB). So, in total 4 models are used in our experimental analysis. We ran the experiment by using 4 different sequences in standard QCIF format (up to 100 frames on each). These are AKIYO, CONTAINER, COASTGUARD and FOREMAN. Then, we simulated 3 sets of Signal to Noise Ratio (SNR) levels in AWGN. They are:

- 25 dB (low noise)
- 20 dB (medium noise)
- 15 dB (high noise)

Thus, 16 sequences in total are used in our experiment (4 sequences × (1 original clear + 3 set of AWGN)).

For local based optical flow, we set a global smoothness and used a four-point mean differences mask coefficient for gradient determination with a spatial locale window (5×5) at 5 iteration loops without a pyramid.

For BD and BB, we set β = 0.0001, and pre-defined neighborhood (s_i) = ±1.

Finally, the performances analysis was evaluated by using SSIM and EVM.

For SSIM, we reconstructed the image on a specific frame from the result MV (F) of each model and compared with the original ground truth image (T) frame where the higher value meant better performance.

$$SSIM(T,F) = \left(\frac{(2\mu_T\mu_F + c_1)(2\sigma_{TF} + c_2)}{(\mu_T^2 + \mu_F^2 + c_1)(\sigma_T^2 + \sigma_F^2 + c_2)} \right) \quad (9)$$

where μ_T and μ_F are the average of image T and F. σ^2 is variance and σ_{TF} is covariance. C_1 and C_2 are variables to stabilize the division with weak denominator.

For EVM, we calculated with root-mean-square by average with the number of non-zero movement vector of ground truth vector where the lower value meant better performance.

5. Experiment results

Figure 2 illustrates the image frame no. 50 of AKIYO, CONTAINER, COASTGUARD, and FOREMAN sequences when they are contaminated with AWGN at differences level. The average SSIM and EVM over 100 frames of each sequence are aggregated in Table 1 and Table 2 where the values in SSIM and EVM of the best performance for each experiment group are highlighted in red. Figure 3 shows the reconstructed images in frame no. 26 with the resultant MV from the optical flow of each method. Figures 4 to 11 show the graph of SSIM and EVM frame by frame (frame no.1 to frame no.100) under different levels of AWGN.

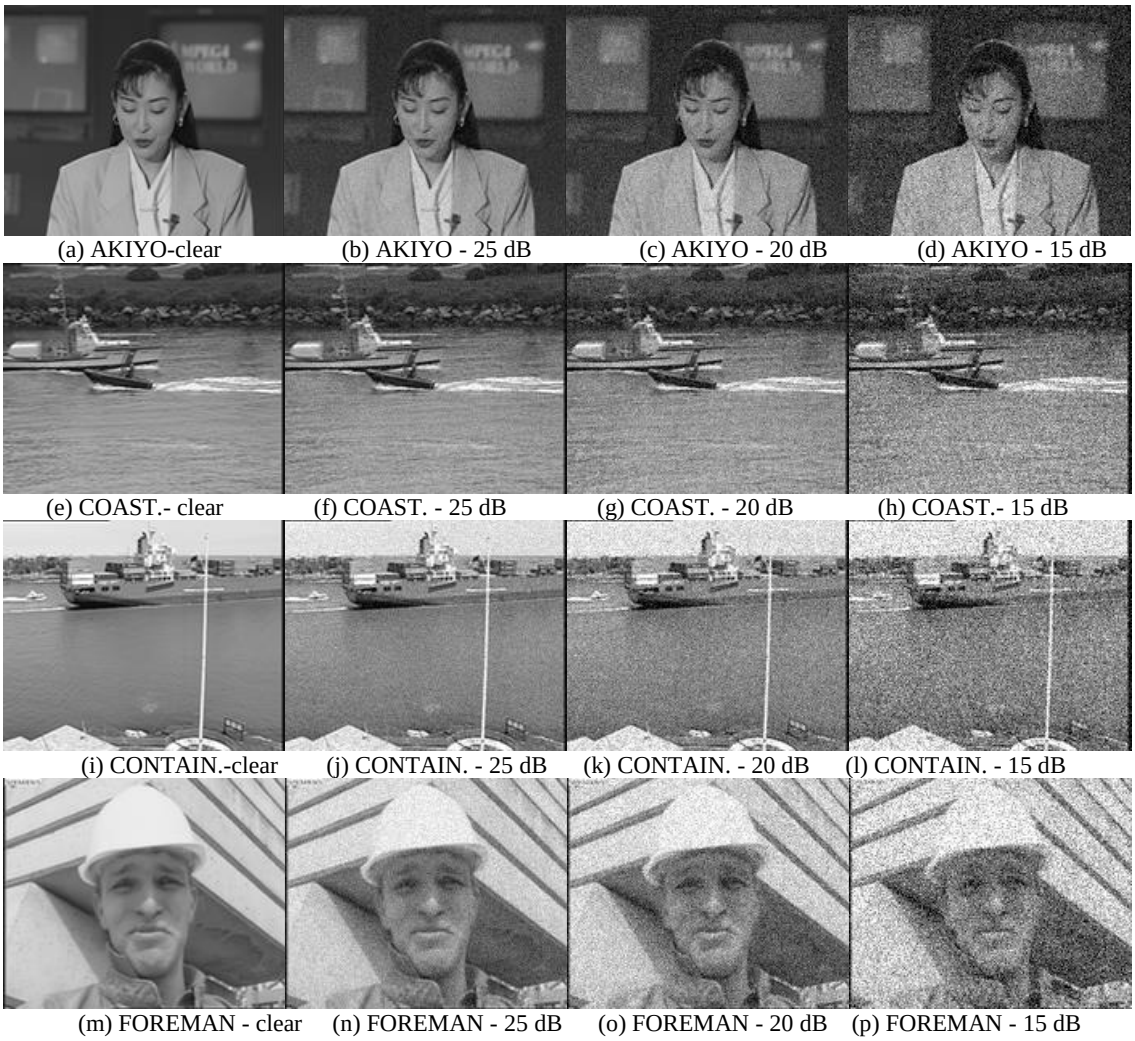

(a) AKIYO-clear (b) AKIYO - 25 dB (c) AKIYO - 20 dB (d) AKIYO - 15 dB

(e) COAST.- clear (f) COAST. - 25 dB (g) COAST. - 20 dB (h) COAST.- 15 dB

(i) CONTAIN.-clear (j) CONTAIN. - 25 dB (k) CONTAIN. - 20 dB (l) CONTAIN. - 15 dB

(m) FOREMAN - clear (n) FOREMAN - 25 dB (o) FOREMAN - 20 dB (p) FOREMAN - 15 dB

Figure 2 Example of image frame contaminated by AWGN

RJAS Vol. 6 No. 2 Jul.-Dec. 2016, pp. 117-127
ISSN 2229-063X (Print)/ISSN 2392-554X (Online)

Table 1 Average SSIM

		AKIYO		COASTGUARD		CONTAINER		FOREMAN	
		AVG SSIM	SD of SSIM	AVG SSIM	SD of SSIM	AVG SSIM	SD of SSIM	AVG SSIM	SD of SSIM
Clear	LK	0.9787	0.0119	0.6845	0.1198	0.9749	0.0018	0.7929	0.0635
	BD	0.9820	0.0113	0.7003	0.1258	0.9801	0.0014	**0.8003**	0.0630
	BF	0.9785	0.0122	0.6999	0.1314	0.9787	0.0017	0.7786	0.0713
	*BB	**0.9834**	0.0116	**0.7169**	0.1381	**0.9852**	0.0012	0.7890	0.0703
AWGN 25dB	LK	0.9483	0.0084	0.7001	0.1234	0.9253	0.0026	0.7983	0.0519
	BD	0.9584	0.0085	0.7199	0.1310	0.9407	0.0022	0.8080	0.0532
	BF	0.9599	0.0086	0.7258	0.1389	0.9438	0.0019	0.8047	0.0592
	*BB	**0.9708**	0.0088	**0.7479**	0.1477	**0.9628**	0.0017	**0.8164**	0.0604
AWGN 20dB	LK	0.9386	0.0069	0.7010	0.1240	0.9061	0.0030	0.8007	0.0482
	BD	0.9508	0.0070	0.7234	0.1328	0.9247	0.0027	0.8125	0.0498
	BF	0.9552	0.0072	0.7327	0.1409	0.9320	0.0024	0.8208	0.0541
	*BB	**0.9679**	0.0074	**0.7577**	0.1505	**0.9541**	0.0020	**0.8338**	0.0557
AWGN 15dB	LK	0.9295	0.0056	0.7004	0.1241	0.8897	0.0036	0.7983	0.0519
	BD	0.9439	0.0057	0.7250	0.1340	0.9114	0.0033	0.8080	0.0532
	BF	0.9510	0.0059	0.7368	0.1425	0.9228	0.0024	0.8369	0.0487
	*BB	**0.9660**	0.0061	**0.7643**	0.1531	**0.9481**	0.0021	**0.8514**	0.0507

Table 2 Average EVM

		AKIYO		COASTGUARD		CONTAINER		FOREMAN	
		AVG EVM	SD of EVM	AVG EVM	SD of EVM	AVG EVM	SD of EVM	AVG EVM	SD of EVM
Clear	LK	3.2922	0.1912	3.3094	0.6404	3.6447	0.1407	4.1163	1.1438
	BD	3.2247	0.1835	3.2440	0.6198	3.5886	0.1294	3.9492	0.8280
	BF	3.0831	0.1673	3.1870	0.5972	3.4936	0.1183	3.8802	0.7991
	*BB	**3.0578**	0.1653	**3.1605**	0.5871	**3.4753**	0.1154	**3.8238**	0.8167
AWGN 25dB	LK	3.1399	0.1863	3.1442	0.6169	3.6152	0.1066	3.6772	0.5994
	BD	3.0688	0.1877	3.0727	0.6036	3.5522	0.1083	3.5866	0.5953
	BF	3.0031	0.1848	3.0146	0.5920	3.4893	0.1061	3.5169	0.5898
	*BB	**2.9706**	0.1865	**2.9820**	0.5846	**3.4575**	0.1072	**3.4703**	0.5872
AWGN 20dB	LK	3.1243	0.2114	3.1054	0.6032	3.6022	0.1018	3.5945	0.5675
	BD	3.0520	0.2143	3.0315	0.5958	3.5393	0.1027	3.5117	0.5692
	BF	2.9858	0.2075	2.9706	0.5885	3.4889	0.0975	3.4388	0.5705
	*BB	**2.9511**	0.2104	**2.9347**	0.5848	**3.4567**	0.0979	**3.3970**	0.5714
AWGN 15dB	LK	3.1013	0.2266	3.0839	0.5729	3.6117	0.1127	3.6772	0.5994
	BD	3.0234	0.2279	3.0078	0.5732	3.5493	0.1127	3.5866	0.5953
	BF	2.9516	0.2243	2.9464	0.5770	3.4933	0.1074	3.3750	0.5675
	*BB	**2.9110**	0.2267	**2.9087**	0.5775	**3.4648**	0.1067	**3.3358**	0.5709

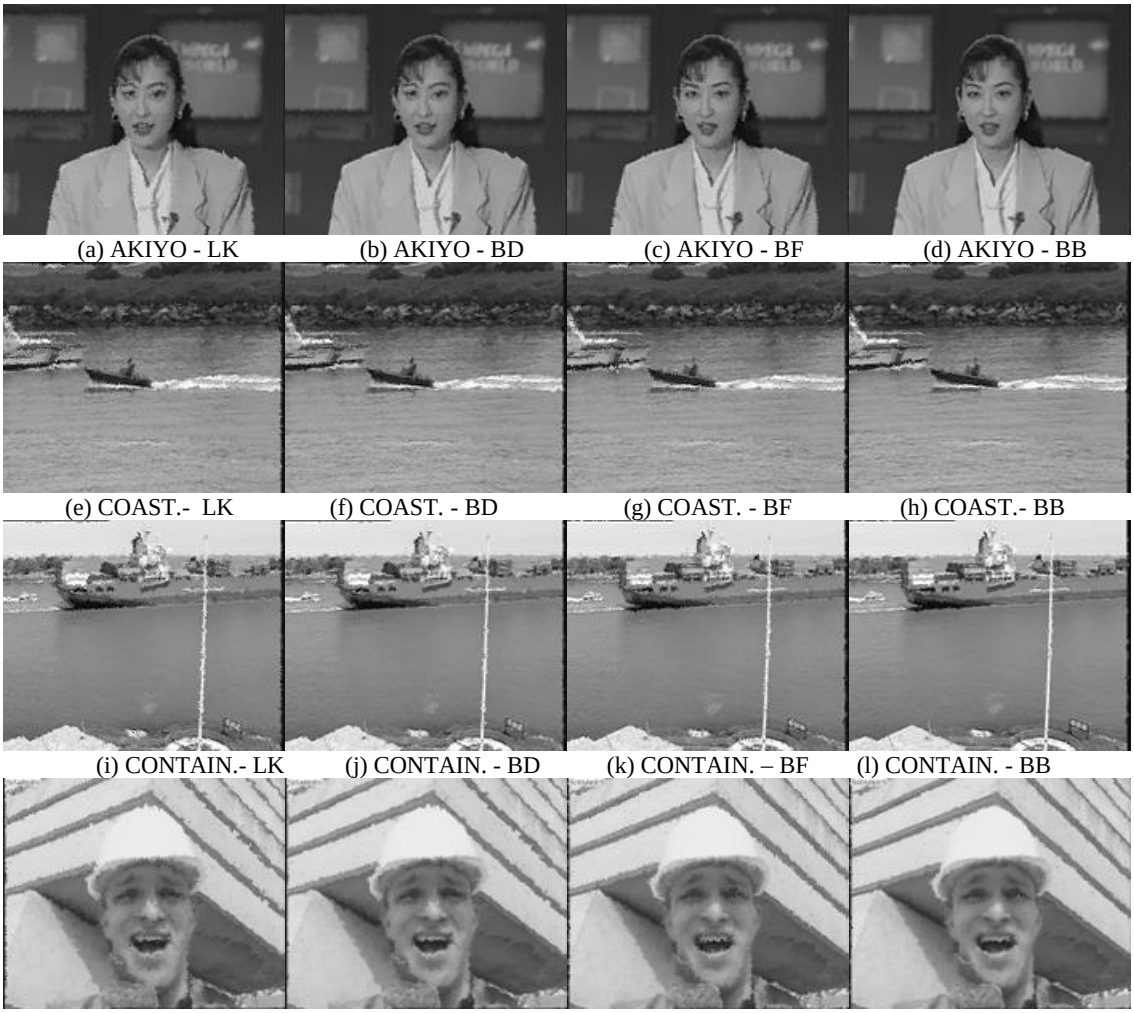

Figure 3 Sample of reconstructed image with optical flow of each method

6. Conclusion

From the experimental results, BD, BF, and BB give better noise tolerances than the traditional local based optical flow on both indices (SSIM and EVM). The results in SSIM, EVM, and quality of reconstructed images indicate that BB presents the best result. In slow motion sequences (AKIYO and CONTAINER), BB presents a significantly higher performance where the deviation is higher than other reference models upon increasing noise levels. Under fast motion sequences (COASTGUARD and FOREMAN), BB still presents the best performance in noise tolerance but shows only slight deviation. BB can present better results because BB focuses on the strength of the bidirectional model and adapts the confidence rate model on the correlation with the bilateral filter to gain better effectiveness in noise tolerance for motion estimation by optical flow.

7. Acknowledgements

This research project was funded by Assumption University.

8. References

Fleet, D. J., & Jepson, A. D. (1990). Computation of component image velocity from local phase information. *International journal of Computer Vision*, *5*(1), 77-104. DOI: 10.1007/BF00056772

Horn, B. K. P., & Schunck, B. G. (1981). Determining optical flow. *Artificial Intelligence*, *17*, 185-203.

Kesrarat, D., & Patanavijit, V. (2010). *Performance evaluation of differential optical flow algorithms based on high confidence reliability with sub-pixel displacement*. Paper presented at The 33rd Engineering Conference (EECON), 1305-1308.

Kesrarat, D., & Patanavijit, V. (2011a). *Experimental performance analysis of high confidence reliability based on differential optical flow algorithms over AWGN sequences with sub-pixel displacement*. Paper presented at IEEE International Symposium on Intelligent Signal Processing and Communication Systems (ISPACS), 1-6.

Kesrarat, D., & Patanavijit, V. (2011b). *A novel robust and high reliability spatial correlation optical flow algorithm based on median motion estimation and bidirectional symmetry flow technique*. Paper presented at IEEE International Symposium on Intelligent Signal Processing and Communication Systems (ISPACS), 1-6.

Kesrarat, D., & Patanavijit, V. (2013). Experimental analysis of performance comparison on both linear filter and bidirectional confidential technique for spatial domain optical flow algorithm. *The ECTI Transactions on Computer and Information Technology (ECTI-CIT), 7*(2), 157-168.

Kesrarat, D., & Patanavijit, V. (2015). *Bidirectional confidential with bilateral filter on local based optical flow for image reconstruction under noisy condition*. Paper presented at IEEE/ACIS International Conference on Software Engineering, Artificial Intelligence, Networking and Parallel/Distributed Computing (SNPD), 1-4.

Kondo, T., & Kongpawechnon, W. (2009). Robust motion estimation methods using gradient orientation information. *ScienceAsia 35 (Journal of The Science Society of Thailand)*, 196-202.

Li, R., & Yu, S. (2008). *Confidence based optical flow algorithm for high reliability*. Paper presented at the IEEE International Conference on Acoustics, Speech, and Signal Processing (ICASSP), 785-788.

Lucas, B. D., & Kanade, T. (1981). An iterative image registration technique with an application to stereo vision. *Proceedings of Defense Advanced Research Projects Agency (DARPA) Image Understanding Workshop*, 121-130.

Mozerrov, M. G. (2013). Constrained optical flow estimation as a matching problem. *IEEE Transactions on Image Processing, 2*(5), 2044-2055.

Paris, S., Kornprobst, P., Tumblin, J., & Durand, F. (2008). Bilateral filtering: Theory and applications..*Foundation and Trends in Computer Graphics and Vision, 4*(1), 1-73. DOI: 10.1561/0600000020

Reed, T. R. (2005). *Digital image sequence processing, compression, and Analysis*. Broca Raton, Fl., USA: Chemical Rubber Company (CRC) Press.

Sun, J., Li, Y., Kang, S., & Shun, H.-Y. (2005). *Symmetric stereo matching for occlusion handling*. Paper presented at IEEE Conference in Computer Vision and Pattern Recognition, 399-406.

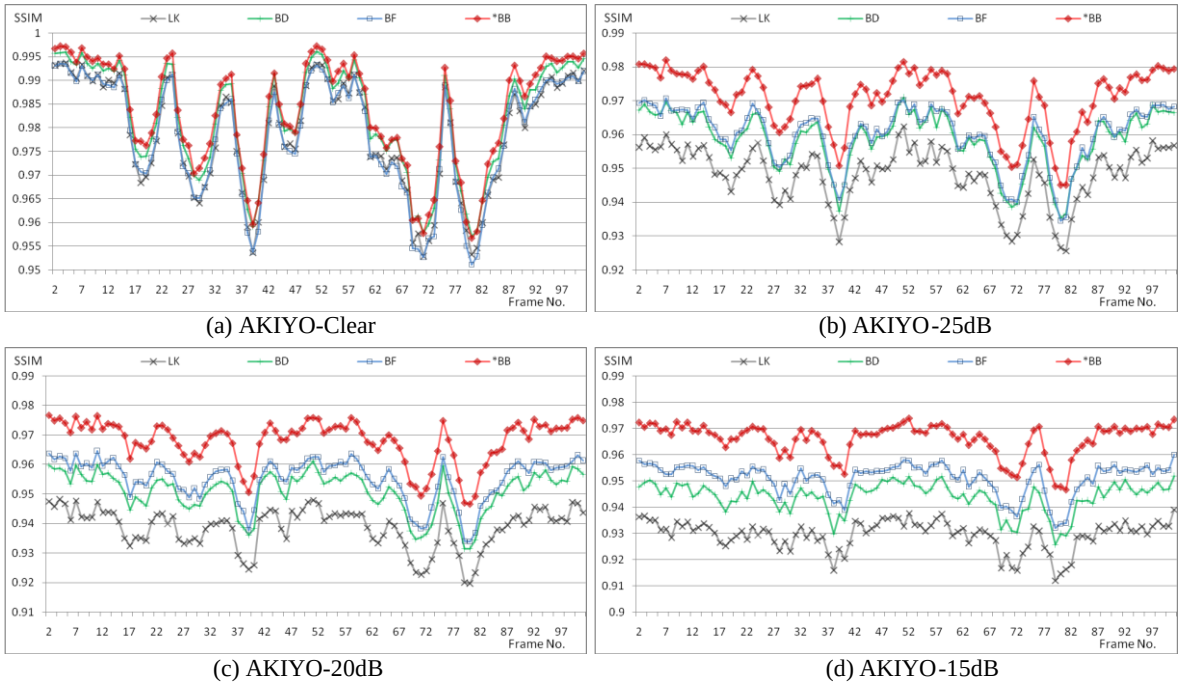

(a) AKIYO-Clear (b) AKIYO-25dB

(c) AKIYO-20dB (d) AKIYO-15dB

Figure 4 SSIM frame by frame in AKIYO sequence

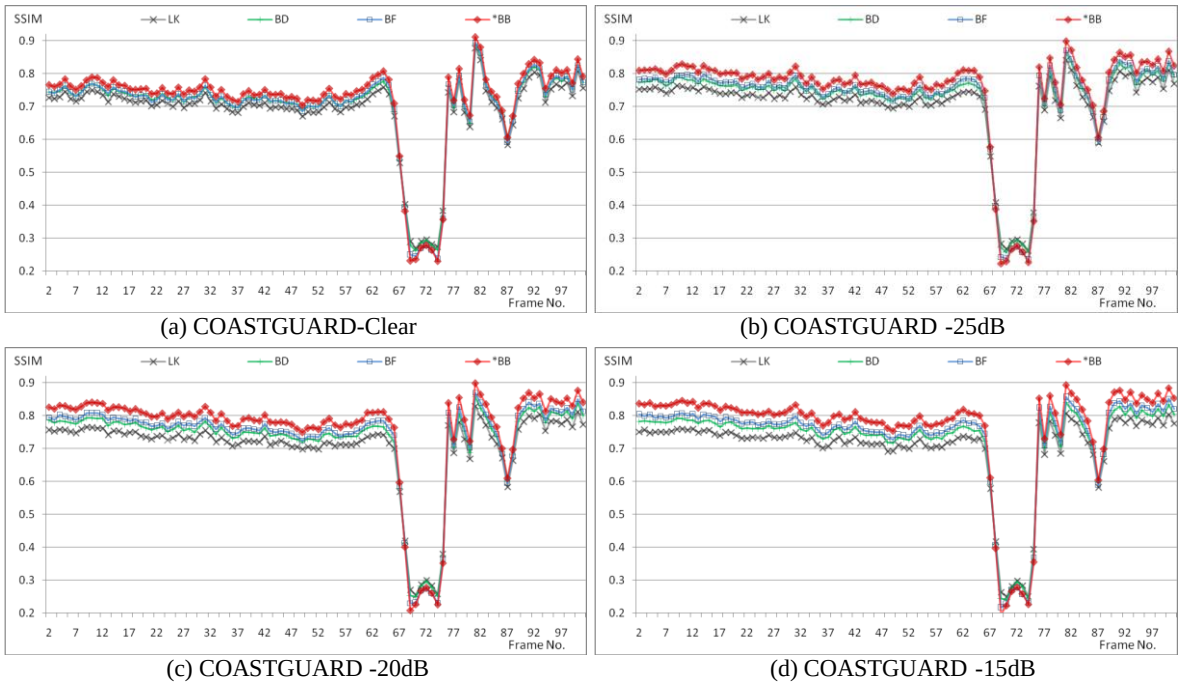

(a) COASTGUARD-Clear (b) COASTGUARD -25dB

(c) COASTGUARD -20dB (d) COASTGUARD -15dB

Figure 5 SSIM frame by frame in COASTGUARD sequence

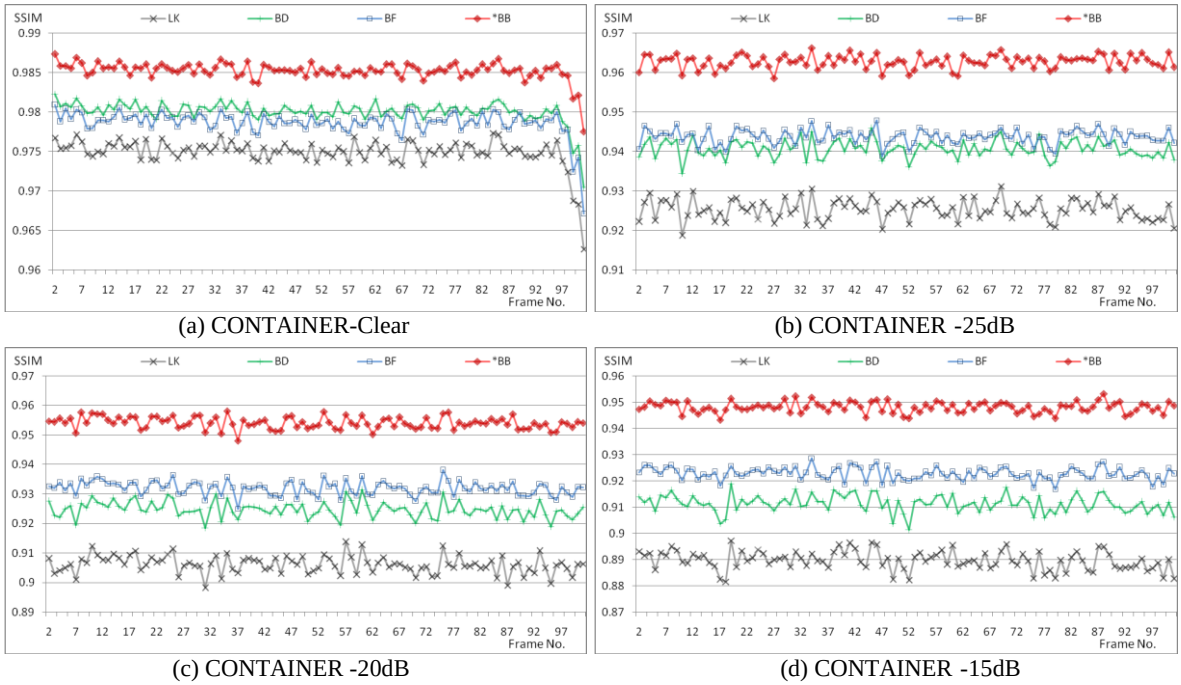

(a) CONTAINER-Clear (b) CONTAINER -25dB

(c) CONTAINER -20dB (d) CONTAINER -15dB

Figure 6 SSIM frame by frame in CONTAINER sequence

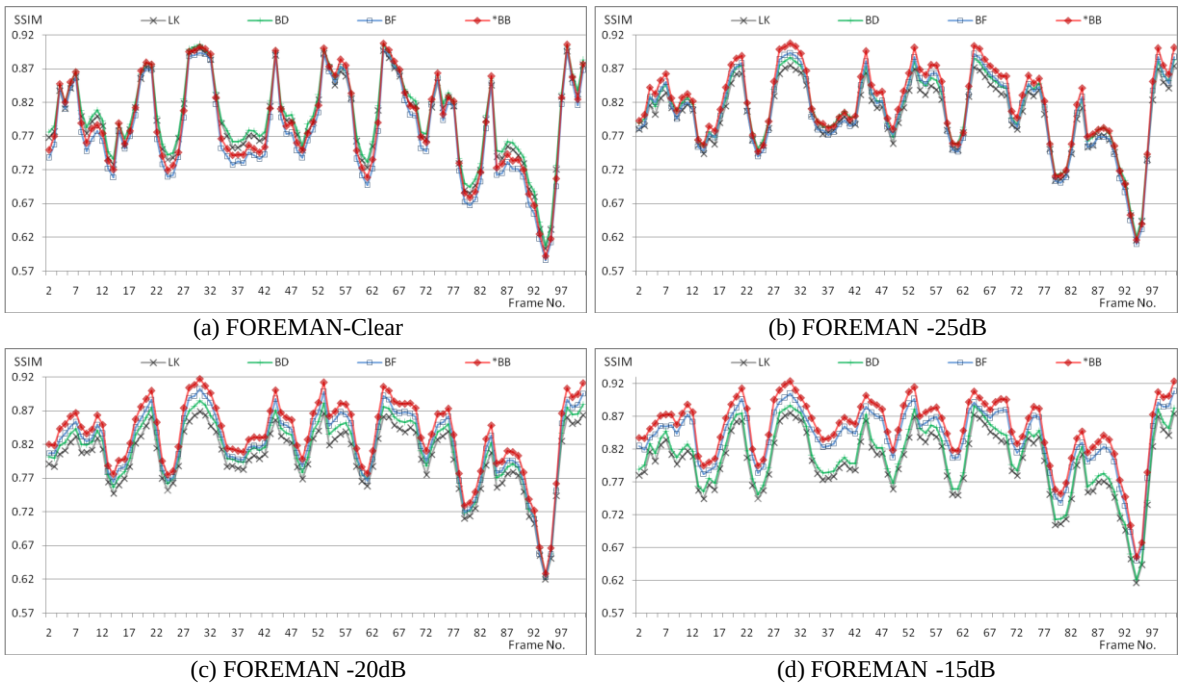

(a) FOREMAN-Clear (b) FOREMAN -25dB

(c) FOREMAN -20dB (d) FOREMAN -15dB

Figure 7 SSIM frame by frame in FOREMAN sequence

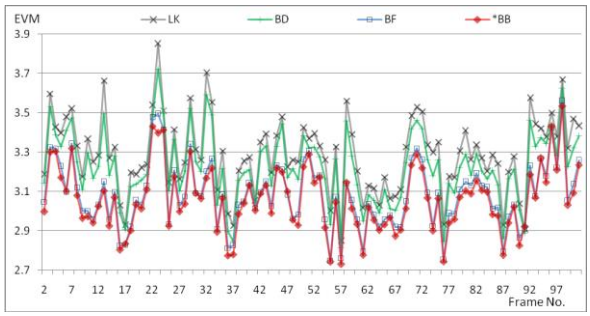

(a) AKIYO-Clear

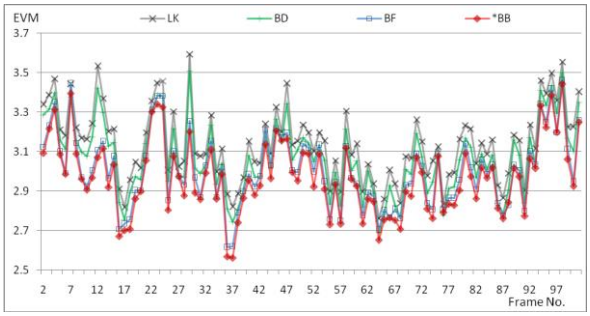

(b) AKIYO-25dB

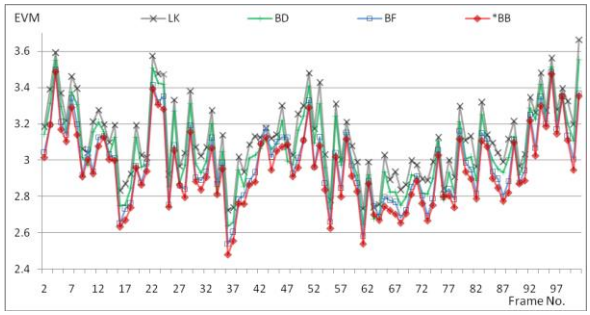

(c) AKIYO-20dB

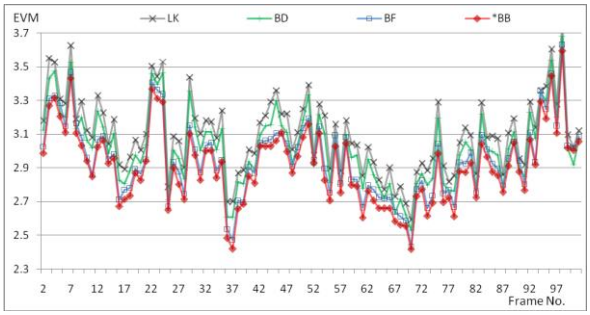

(d) AKIYO-15dB

Figure 8 EVM frame by frame in AKIYO sequence

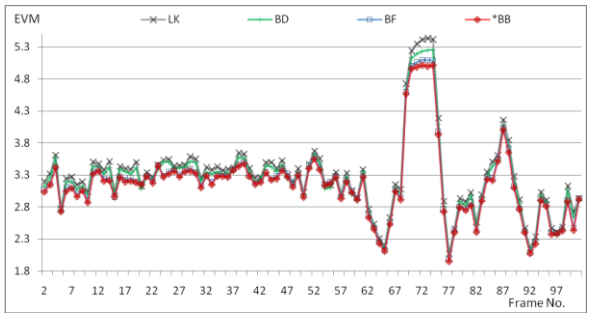

(a) COASTGUARD-Clear

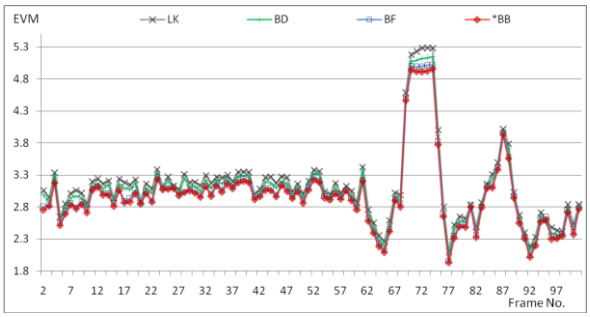

(b) COASTGUARD -25dB

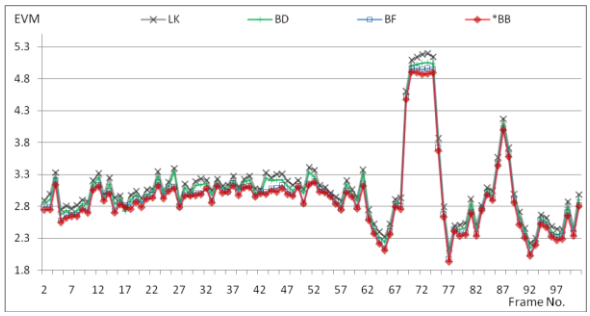

(c) COASTGUARD -20dB

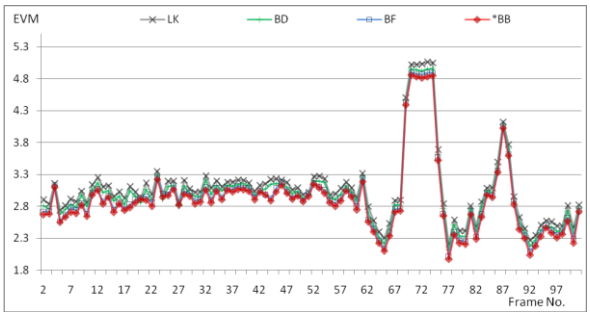

(d) COASTGUARD -15dB

Figure 9 EVM frame by frame in COASTGUARD sequence

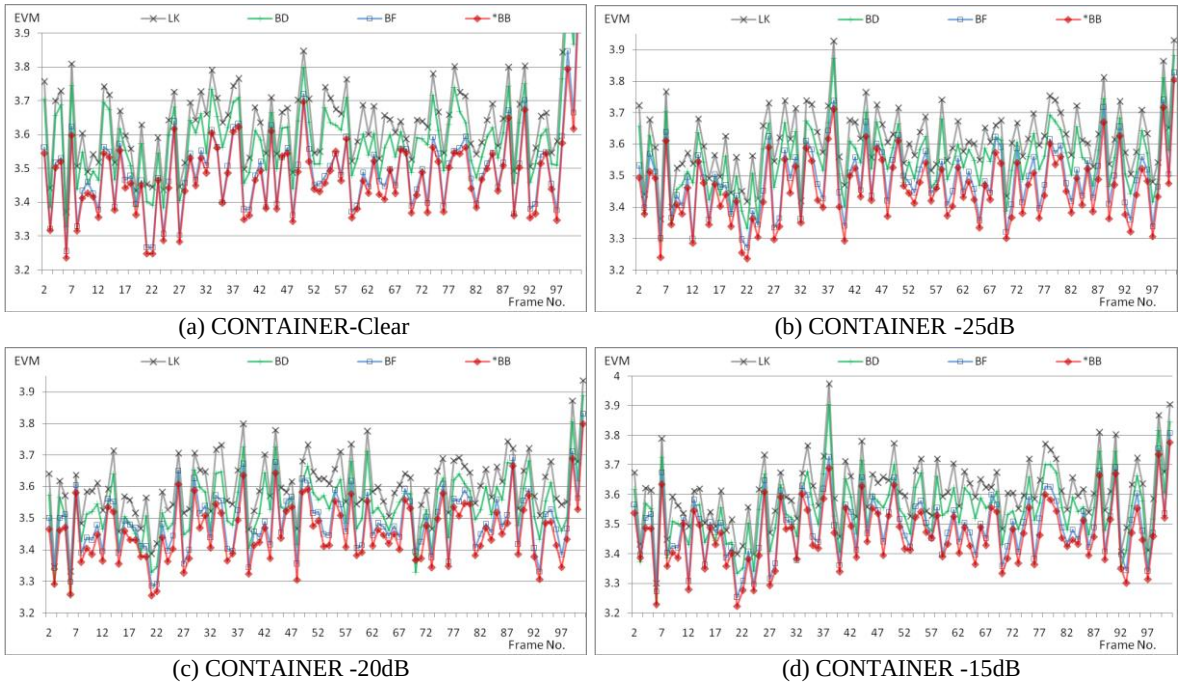

(a) CONTAINER-Clear (b) CONTAINER -25dB

(c) CONTAINER -20dB (d) CONTAINER -15dB

Figure 10 EVM frame by frame in CONTAINER sequence

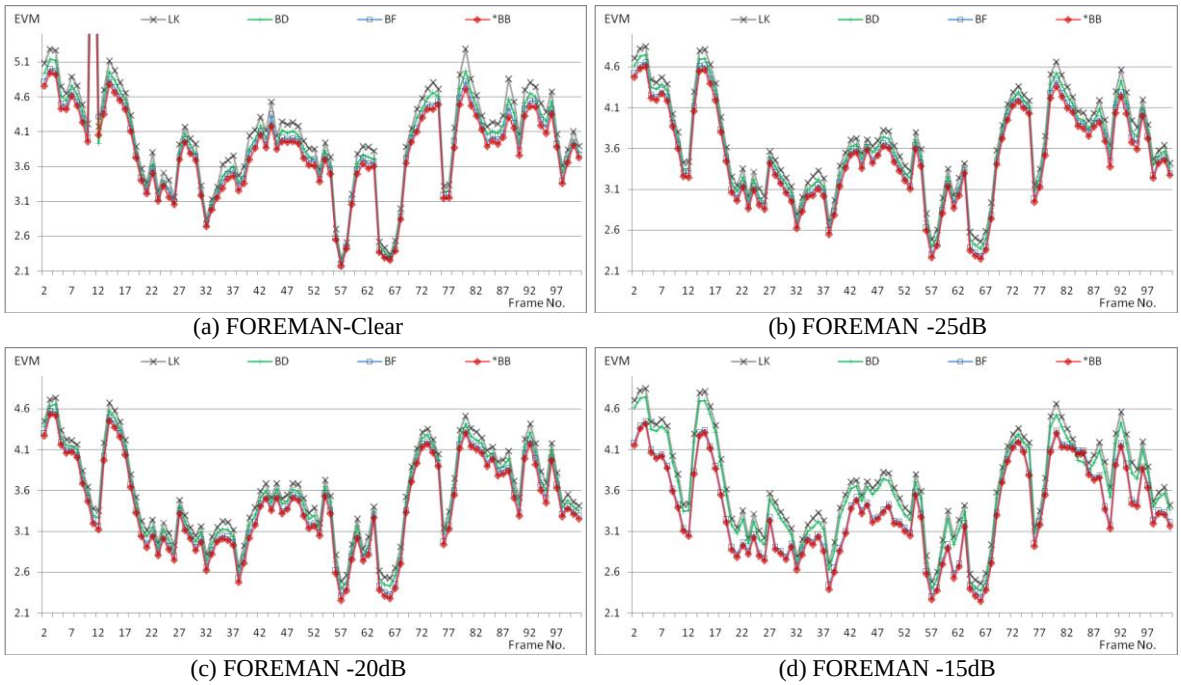

(a) FOREMAN-Clear (b) FOREMAN -25dB

(c) FOREMAN -20dB (d) FOREMAN -15dB

Figure 11 EVM frame by frame in FOREMAN sequence